Synthesis, Characterization, and Application of Composite Alginate Microspheres with Magnetic and Fluorescent Functionalities

Jiwei Liu,[1,2] Yu Zhang,[1] Ting Yang,[1,2] Yuqing Ge,[1] Song Zhang,[1] Zhongping Chen,[1,2] Ning Gu[1]

[1]*State Key Laboratory of Bioelectronics, Jiangsu Key Laboratory for Biomaterials and Devices, Nanjing 210096, People's Republic of China*
[2]*School of Chemistry and Chemical Engineering, Southeast University, Nanjing 210096, People's Republic of China*

Received 9 April 2008; accepted 22 March 2009
DOI 10.1002/app.30487
Published online 27 May 2009 in Wiley InterScience (www.interscience.wiley.com).

ABSTRACT: Composite alginate microspheres were synthesized via a modified emulsification technique and characterized by inverted optical microscope, transmission electron microscope, ζ-potential analyzer, UV–vis spectrophotometer, luminescence spectrometer, and vibrating sample magnetometer. The results show that the synthetic parameters including the weight ratio of maghemite nanoparticles to alginate, hydrophile-lipophile balance (HLB) value, stirring speed, and $CaCl_2$ dripping rate play important roles in the synthesis of microspheres. Furthermore, the composite alginate microspheres exhibit good superparamagnetism and fluorescence, which can serve both as magnetic resonance contrast agents and optical probes for biological imaging. © 2009 Wiley Periodicals, Inc. J Appl Polym Sci 113: 4042–4051, 2009

Key words: alginate microspheres; crosslinking; emulsification; fluorescence; magnetic nanoparticles

INTRODUCTION

Over the past decade, iron oxide nanoparticles (NPs) consisting of maghemite (γ-Fe_2O_3) or magnetite (Fe_3O_4) have been of great interest and importance not only because of their unique properties but also due to their potential applications in biomedical fields such as cell separation,[1,2] magnetic resonance imaging (MRI),[3,4] drug delivery systems,[5] and hyperthermia.[6] Most of these applications require the magnetic NPs to be chemically stable and well dispersed. However, it has been demonstrated that surface modification of NPs could help prevent their aggregation and improve their chemical stability.[7–9] One of the more feasible routes is to embed or encapsulated magnetic NPs in polymer matrix with controllable structures. Up to now, composite particles consisting of magnetic NPs embedded or encapsulated in polymer matrix (e.g., polystyrene,[10–12] chitosan,[13,14] and albumin[15]) have been reported by several authors. Nevertheless, the as-synthesized composite particles based on these synthetic polymers or biopolymers have some drawbacks such as expensiveness, time-consuming preparation, low stability, complicated isolation and purification, and low magnetic sensitivity, which restrict their further applications.

Alginate, a well-known naturally occurring polysaccharide, is composed of guluronic and mannuronic acid residues which vary in composition and sequence depending on the source of the alginate. Because of its unique properties including inexpensiveness, biocompatibility, a relatively inert hydrogel environment within the matrix and a mild room temperature encapsulation process, alginate has attracted intense attention as an important class of biomaterial in recent years.[16] Moreover, alginate can be ionically crosslinked in the presence of divalent cations such as Ca^{2+}, which has been extensively investigated for many biomedical applications such as tissue engineering,[17,18] drug delivery vehicles,[19,20] and cell transplantation matrices.[21]

In pioneer work, Kroll and Winnik[22] have reported the method for the preparation of magnetic alginate that uses the crosslinking ion of Fe^{2+} or Fe^{3+} as the reaction center for the formation of γ-Fe_2O_3. Llanes et al.[23] have synthesized magnetic nanostructured maghemite-alginate composites with nanocrystallines of maghemite inside the alginate matrix. A similar method has been used to embed iron oxide NPs in alginate

Correspondence to: Y. Zhang or N. Gu (zhangyu@seu.edu.cn or guning@seu.edu.cn).

Contract grant sponsor: National Natural Science Foundation of China; contract grant numbers: 30870679, 50872021, 90406023.
Contract grant sponsor: National Basic Research Program of China; contract grant numbers: 2006CB933206, 2006CB705602.
Contract grant sponsor: Qing Lan Project.

hydrogel by dropping sodium alginate solution into aqueous chloride solution.[24,25] Although there are extensive studies mentioned above, synthesis of magnetic form of alginate is yet a challenging and promising subject. Very recently, magnetic alginate microspheres have been applied for separation and purification of various starch-degrading enzymes such as α-amylases[26] and β-amylases.[27] Shen et al.[28] have reported the synthesis of ferrofluid alginate microcapsules visible with MRI. Recently, magnetic alginate beads combined with iron oxide NPs and activated carbon have been used to remove organic dyes via a solid-phase extraction process assisted by a magnetic field.[29] As specifically required in biological and biomedical applications, current research has been focused on synthesizing microspheres in submicro-to-micrometer scale with electrical, fluorescent, magnetic, and/or catalytic properties. Therefore, a considerable effort has been devoted to the development of multifunctional microspheres.[10–15,30,31] To our knowledge, none of the study about the synthesis of multifunctional alginate microspheres has been reported so far.

In this article, composite alginate microspheres with magnetic and fluorescent functionalities have been synthesized via an emulsification technique. The influence of the γ-Fe_2O_3-to-algiante weight ratio (*R*), hydrophile-lipophile balance (HLB) value, stirring speed, and $CaCl_2$ dripping rate on the synthesis of the microspheres was investigated. Moreover, the microspheres described here can serve both as magnetic resonance contrast agents for MRI and optical probes for fluorescence microscopy, which will have great potential in a variety of biological and biomedical applications.

EXPERIMENTAL

Materials

Sodium alginate (1 wt %, viscosity ≥0.2 Pas, 20°C), sorbitan trioleate (SPAN 85), polyoxyethylene sorbitan trioleate (TWEEN 85), ferric chloride hexahydrate, ferrous sulfate heptahydrate, ammonia solution, 1,6-diaminohexane, 2-propanol, acetone, sodium acetic, sodium bicarbonate, and calcium chloride were all purchased from Shanghai Chemicals Co. *N*-(3-dimethylaminopropyl)-*N*′-ethylcarbodiimide hydrochloride (EDC), *N*-hydroxysulfosuccinimide sodium salt (NHSS), meso-2,3-dimercaptosuccinic acid (DMSA), and fluorescein isothiocyanate (FITC, isomer I) were obtained from Sigma-Aldrich (Superior Chemical & Instruments Co., LTD., Beijing, China). All chemicals were used as received without further treatment.

Preparation of DMSA-coated γ-Fe_2O_3 (γ-Fe_2O_3@DMSA) NPs

γ-Fe_2O_3 NPs were prepared according to our previous procedure.[32] Briefly, 500 mL aqueous solution of $FeCl_3$ (0.1*M*) and $FeSO_4$ (0.06*M*) was prepared under nitrogen gas, followed by addition of 200 mL ammonia aqueous solution (1.5*M*) with vigorous stirring at room temperature. After 30 min, the resulting Fe_3O_4 were collected by magnetic separation and washed several times with ethanol and water. Then, the Fe_3O_4 NPs were dispersed in water with a mass concentration of 3 mg·mL^{-1} and pH 3.0, and oxidized into reddish-brown γ-Fe_2O_3 NPs under aeration (with air) for 1 h at about 100°C. Subsequently, the γ-Fe_2O_3 NPs were coated with DMSA according to the process described elsewhere.[9,33] Finally, the products were washed repeatedly with water and enriched with the help of a magnet.

Synthesis of alginate-FITC derivative

Alginate-FITC derivative was synthesized according to the process,[34,35] as presented in Scheme 1. Briefly, 12 g 1 wt % sodium alginate aqueous solution was mixed with EDC/NHSS (50 mg/30 mg) for the activation of carbonyl groups on alginate in pH 4.9 sodium acetic buffer for 30 min, followed by addition of 1,6-diaminohexane (60 mg) for another 4 h. The mixture was precipitated in 2-propanol to remove unreacted diamine. The alginate-amine derivative was reacted with FITC (1 mg) in pH 9.0 sodium bicarbonate solution for 4 h and precipitated in acetone. The resulting alginate-FITC derivative was added into mixed aqueous solution of γ-Fe_2O_3@DMSA NPs and sodium alginate, which was then used to synthesize microspheres using the following process.

Synthesis of composite alginate microspheres

As illustrated in Scheme 2, the synthesis of composite alginate microspheres was a modification of the conventional emulsification technique.[34-37] The emulsification process was carried out in a four-neck flask equipped with a stirrer, an ultrasonicator, and a microinfusion pump. Typically, 50 g aqueous solution of γ-Fe_2O_3@DMSA NPs and alginate (R: 0.1) was dispersed in 75 g isooctane containing 1.696 g SPAN 85, ultrasonicating and stirring for 10 min. Then, a solution of 5 g isooctane containing 0.904 g TWEEN 85 was added to the emulsion under stirring and ultrasonication at the same power for 20 min. After that, another 30 mins of stirring was proceeded to achieve stable water-in-oil emulsion droplet. Subsequently, 20 mL of aqueous solution containing 10 wt % of calcium chloride was added by the microinfusion pump to form ionic crosslinks. Finally, the products were washed with water by magnetic decantation for four times and redispersed into water at room temperature.

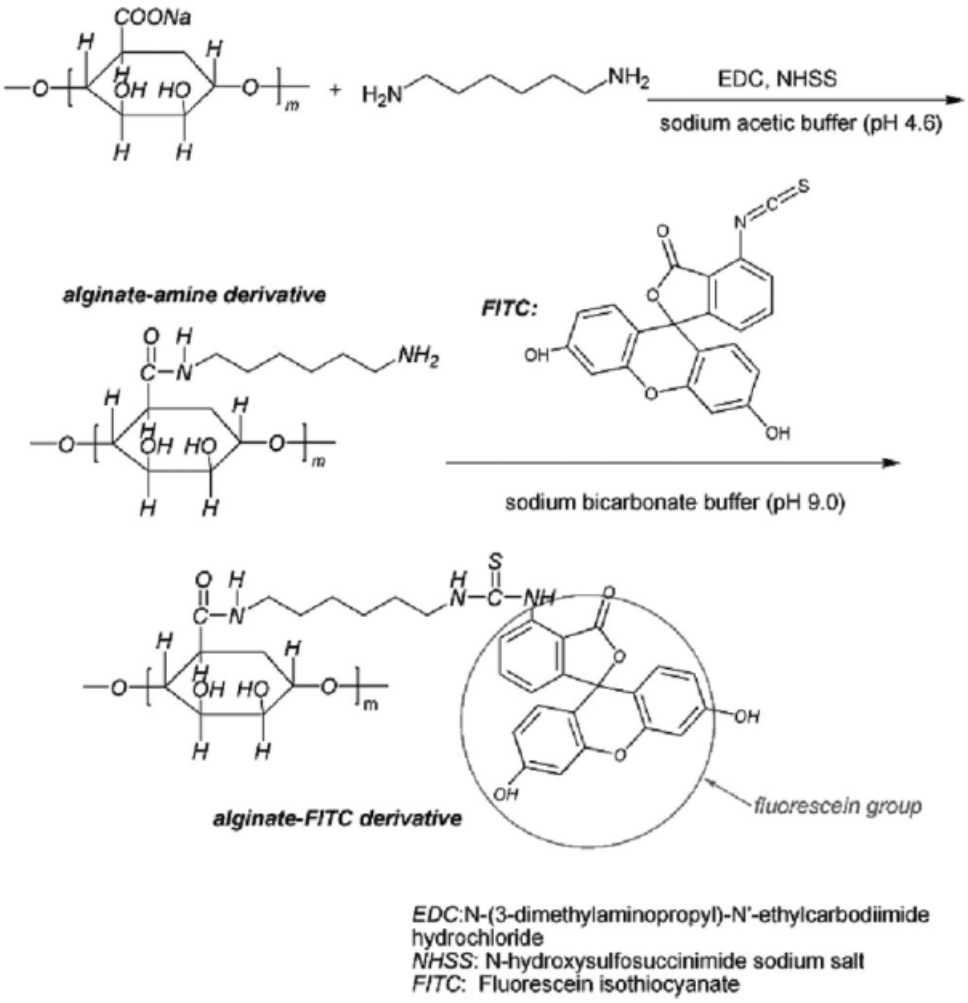

Scheme 1 Procedure for the synthesis of alginate-FITC derivative.

Cell culture and labeling

Macrophage cell line, RAW264.7, was provided by Shanghai Cellular Institute of China Scientific Academy. Cells were cultured in RPMI 1640 medium containing 10% fetal calf serum (FCS), 100 μg/mL penicillin, and 100 μg/mL streptomycin. The cells were incubated at 37°C in 5% CO_2 atmosphere. In cell labeling experiments, the cells were incubated with different concentrations of composite microspheres (~1 μm diameter in size) suspension in medium for 2 h. After particles labeling, adhering cells were washed three times with 0.1*M* PBS and then fixed with 2% glutaraldehyde buffered in 0.1*M* PBS

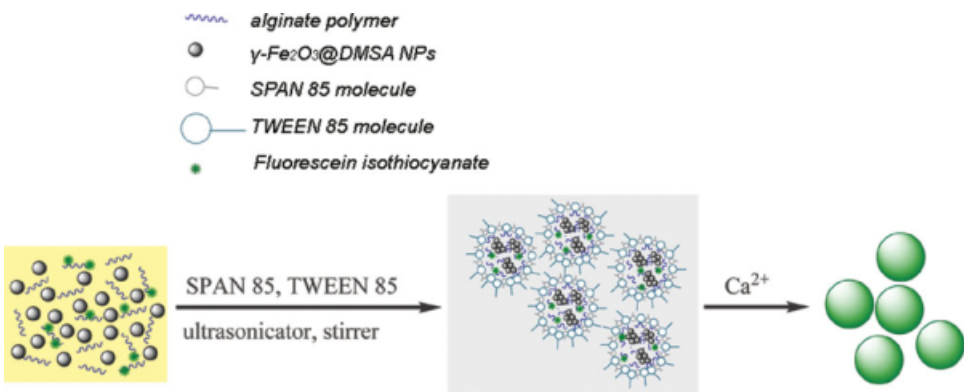

Scheme 2 Schematic illustration of the synthesis of composite alginate microspheres. [Color figure can be viewed in the online issue, which is available at www.interscience.wiley.com.]

for 1 h at 4°C. For control experiments, medium having no particles was used. To determine cell cytotoxicity/viability, the cells were plated at a density of 1×10^5 cells/well in 96-well plates at 37°C in 5% CO_2 atmosphere. After 24 h of culture, the medium in the wells was replaced with the fresh medium containing particles in the concentration range of 0–0.1 mg/mL. After 2 h, the medium was removed and rinsed with medium, and then 20 μL of MTT (3,4,5-dimethylthiazol-yl-2,5-diphenyl tetrazolium) dye solution (5 mg/mL in medium) was added to each well. After 4 h of incubation at 37°C in 5% CO_2 atmosphere, the medium was removed, and Formazan crystals were dissolved in 200 μL dimethylsulfoxide (DMSO) and quantified by measuring the absorption of the solution at 570 nm by a microplate reader (Model 680, Bio-Rad, Richmond, CA). The relative cell viability (%) related to control wells containing cell culture medium without particles was calculated.

Characterizations

The shape of the microspheres was determined by inverted optical microscope (Zeiss, Axioscop200). Size distribution was measured by quasi-elastic light scattering (Malvern Mastesizer 2000). The diameter measurements were performed at 20°C and angles of 45°, 60°, 90° after dilution in water. The morphology of the microspheres was characterized by transmission electron microscope (TEM, JEOL, JEM-2000EX). The samples were prepared by dropping 6 μL of solution on the carbon-coated copper grids and allowing the solution to dry in the air. Powder X-ray diffraction (XRD, Rigaku, D/MaxRA, $\lambda = 1.5405 \times 10^{-10}$ m, CuKα) and selected-area electron diffraction (SAED) were used to determine the crystal structure of the products. The surface charge of the products was investigated through ζ-potential analyzer (Beckman Coulter, Delsa 440SX, Germany). The ζ-potential measurements were performed in water at different pH value adjusted with 0.1*M* HCl and NaOH solution. UV–vis absorption spectra were acquired using an UV–vis-NIR spectrophotometer (UV-3150, SHIMADZU) with a scan speed of 200 nm/min. Fluorescence spectra were measured on luminescence spectrometer (LS 55, PerkinElmer, Palo Alto, CA) equipped with a Xenon lamp. The samples were contained in a 1-cm quartz cuvette and illuminated using the excitation wavelengths of 490 nm for FITC (slit width: 5.0 nm). The fluorescence images were taken on a fluorescence inverted microscope (Zeiss, Axioscop200) excited by Hg lamp. Photoluminescence quantum yield value was measured relative to Rhodamine 590 in water and were calculated using the following equation: $\varphi_f = \varphi f'(I/I')(A'/A)$ (1),[38] where I(sample) and I'(standard) are the integrated emission peak areas, A(sample) and A' (standard) are the absorptions at the excitation wavelength. Magnetic properties were determined with vibrating sample magnetometer (VSM, Lakeshore 7407) at room temperature in a field up to 5 kOe. The optical and fluorescent images of the cells were observed with an Axioskop 200 microscope equipped with a Coolsnap MP3.3 camera (Carl Zeiss, Germany). MRI experiments were conducted using a 1.5 T MR spectrometer (Marconi Elipse). Samples for imaging were prepared by suspending 1×10^6 cells in warm 1.0% agarose gel. Gradient echo acquisition parameters for T_2*-weighted imaging were as follows: repetition time/echo times (T_R/T_E) = 520 ms/17.90 ms, flip angle = 35°, an acquisition matrix of 256 × 256, filed of view of 10 × 10 cm, section thickness of 2 mm, and 4 averages. Region of interest for signal intensity measurement was 20 mm^2. Another two Eppendorf tubes containing 1×10^6 unlabeled cells and distilled water were used.

RESULTS AND DISCUSSION

Preparation of γ-Fe_2O_3@DMSA NPs

γ-Fe_2O_3@DMSA NPs, selected as magnetic cores, were prepared by chemical coprecipitation. The stable ferrofluid was obtained via surface modification with DMSA. Figure 1(a) shows the TEM image of the γ-Fe_2O_3@DMSA NPs, most of which are approximately spherical with an average diameter of 18 nm. According to the SAED pattern [inset in Fig. 1(a)], the *d*-spacing can be calculated in the following equation: $L\lambda = dR$ **(2)**, where L is the distance between the test sample and the film (L = 137 cm), λ is the wavelength of electron beam (λ= 0.0251 Å), R is the radius of the diffraction ring. The calculation results are shown in Table I, which experimentally accord with the results obtained from XRD pattern [Fig. 1(b)]. These results indicate the inverse cubic spinel structure of the γ-Fe_2O_3@DMSA NPs. As shown in Figure 2(a), the γ-Fe_2O_3@DMSA NPs have high negative potential at a wide range of pH value, which are more stable due to the strong electrostatic repulsion. On the other hand, the γ-Fe_2O_3 NPs modified with DMSA possess high hydrophilicity, which is attributed to the carboxyl groups of the DMSA molecules. Thus, the γ-Fe_2O_3@DMSA NPs were used as magnetic cores for the synthesis of composite microspheres.

Synthesis of alginate-FITC derivative

Figure 3 shows the UV–vis absorption spectra of free FITC, alginate-FITC derivative and alginate. The original alginate did not display any characteristic absorption between 400 and 600 nm. However,

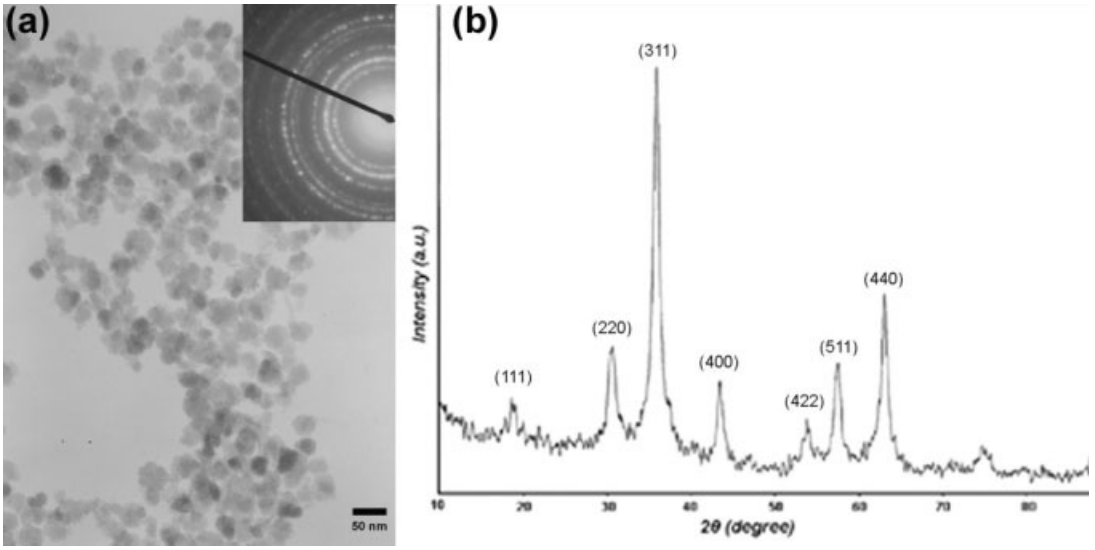

Figure 1 TEM image (a) and XRD pattern (b) of the γ-Fe_2O_3@DMSA NPs. The insert in (a) shows a typical SAED pattern.

alginate-FITC derivative possessed strong absorption at 488 nm, attributed to the absorption of the fluorescein group of organic molecule FITC (see red circle in Scheme 1), which confirmed the successful synthesis of alginate-FITC derivative. Moreover, a series of solutions of different concentrations of alginate-FITC derivative were measured with UV–vis spectroscopy, demonstrating the relationship between the absorption and concentration (inset in Fig. 3).

Synthesis of composite alginate microspheres

To study the effect of synthetic parameters on the synthesis of composite microspheres, a series of microspheres were synthesized by changing the *R*, HLB value, stirring speed, and $CaCl_2$ dripping rate. Figure 4 shows that the size of the microspheres decreased with increasing *R* and HLB value and stirring speed and with decreasing $CaCl_2$ dripping rate. And a significant increase in the size of microspheres was noted when the HLB value and stirring speed were decreased to 3 and 400 rpm, respectively [Fig. 4(b,c)]. Especially, nonspherical particles were obtained when the *R* was increased to 0.5 [Fig. 5(a)]. This is probably due to the strong dipole–dipole interactions between γ-Fe_2O_3 NPs by increasing their concentration in the alginate matrix. Further investigation indicates that the nonspherical particles can orientate and align along the direction of the applied magnetic field generated by a 0.3 T Nd-Fe-B magnet [Fig. 5(b,c)]. However, the phenomenon of the spherical particles is not as visible as that of the nonspherical ones [Fig. 5(d)]. It is believed that stronger dipolar attraction drives nonspherical particles to align into necklace structure due to their anisotropy compared with the spherical ones, revealing high magnetic sensitivity and manipulability under an external magnetic field. In addition, the applied Nd-Fe-B magnet, with a distance of 15 cm away from the sample, may be responsible for weaker dipolar attraction, which could not drive spherical particles to align along the direction of the applied magnetic field. The average length of the necklacelike structures is several tens of micrometers, whereas the average width is several hundreds of nanometers [see inset in Fig. 5(d)].

Characterization of composite alginate microspheres

Figure 6 shows a typical optical microscopy image of the microspheres and corresponding diameter

TABLE I
XRD and SAED Data for the γ-Fe_2O_3@DMSA NPs

	1	2	3	4	5	6	7
R (cm)	0.78	1.27	1.48	1.79	2.20	2.33	2.53
SAED results-*d* (Å)	4.44	2.71	2.32	1.92	1.56	1.48	1.36
XRD results-*d* (Å)	4.67	2.90	2.49	2.06	1.70	1.60	1.47
Theory values-*d* (Å)	4.82	2.95	2.51	2.09	1.70	1.61	1.47
Crystalline plane (hlk)	(111)	(220)	(311)	(400)	(422)	(511)	(440)

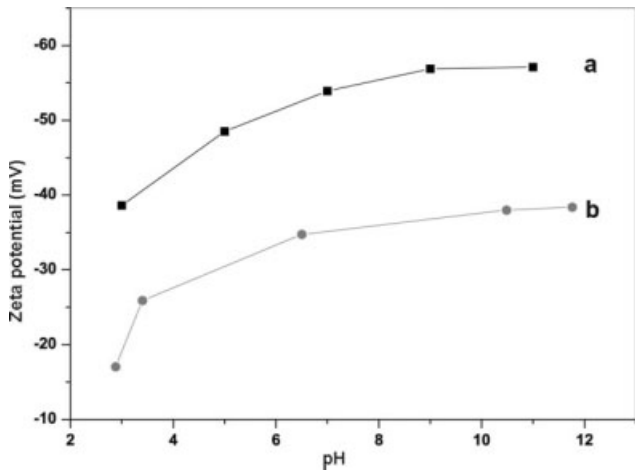

Figure 2 ζ-potential measurements for the γ-Fe_2O_3@DMSA NPs (a) and composite alginate microspheres (b) at different pH value.

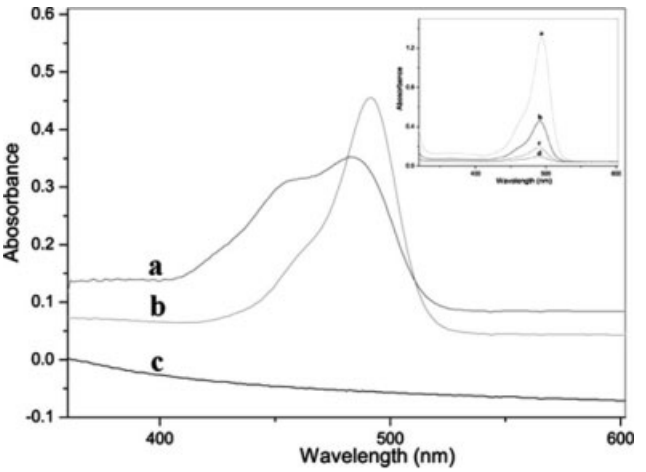

Figure 3 UV–vis absorption spectra of free FITC (a), alginate-FITC derivative (b), and alginate (c). Inset: UV–vis absorption spectra of alginate-FITC derivative solutions diluted by zerofold (a), threefold (b), ninefold (c), and 27-fold (d), respectively.

distribution. Alginate microspheres with mean diameter of 3.56 ± 0.48 μm were obtained. The microspheres were found to be stable, and exhibited negative surface charge [Fig. 2(b)]. TEM images in Figure 7(a,b) reveal that the microspheres possess an average diameter of 800 nm. Moreover, the γ-Fe_2O_3 NPs are clearly seen in the dark-field image of

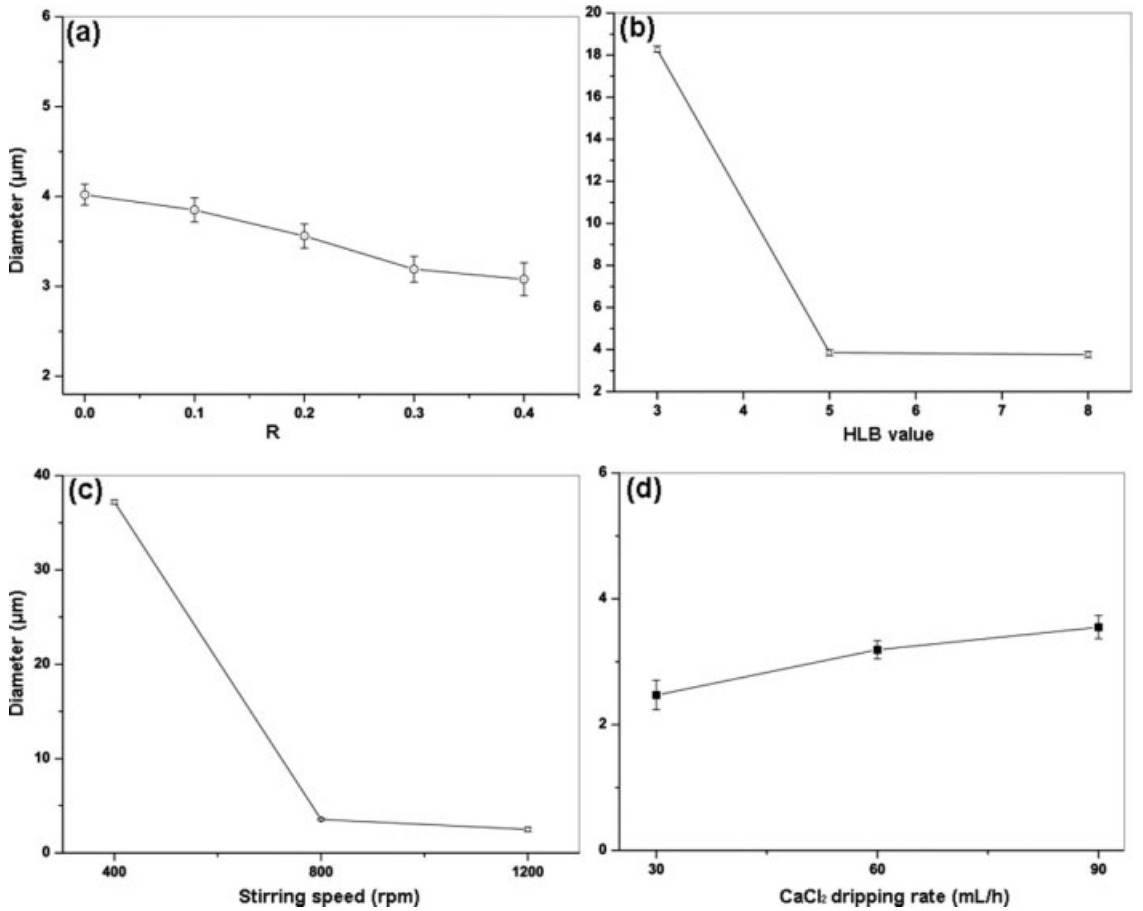

Figure 4 Effect of *R* (a), HLB value (b), stirring speed (c), and $CaCl_2$ dripping rate (d) on the size of composite microspheres. Fixed HLB value (5), stirring speed (800 rpm) and $CaCl_2$ dripping rate (60 mL· h^{-1}) were used in (a). Fixed *R* (0.1), stirring speed (800 rpm), and $CaCl_2$ dripping rate (60 mL· h^{-1}) were used in (b). Fixed *R* (0.2), HLB value (5), and $CaCl_2$ dripping rate (60 mL· h^{-1}) were used in (c). Fixed *R* (0.3), HLB value (5), and stirring speed (800 rpm) were used in (d).

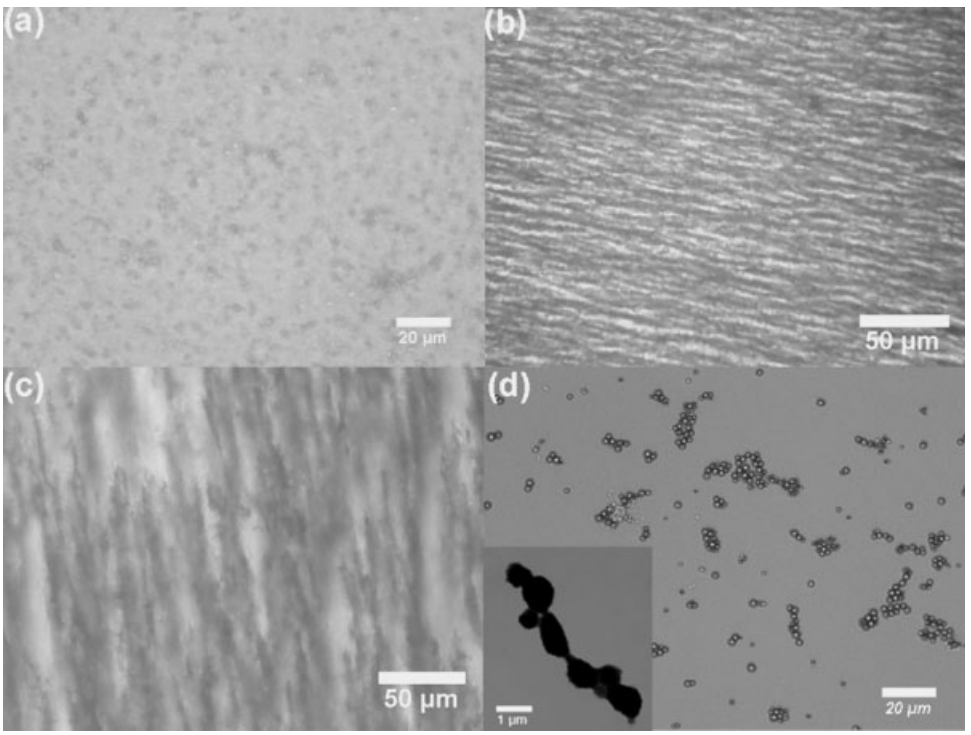

Figure 5 Optical microscopy images of the nonspherical particles in the absence (a) and presence of horizontally (b) and vertically (c) applied magnetic field, and spherical particles in the presence of a vertically applied magnetic field (d). Inset shows a typical TEM image of aligned necklace structure.

Figure 7(c), whereas no free γ-Fe_2O_3 NPs is observed outside the microspheres. Note that the shrinkage of the microspheres took place when prepared for TEM measurement, and this explains why the size of the microspheres in the TEM image is significantly smaller than that in the optical microscopy image. Significantly, the microspheres maintained their spherical form during the shrinkage displaying excellent mechanical property, which is probably due to the encapsulation of a large number of γ-Fe_2O_3 NPs in the microspheres.

Figure 8 shows the room temperature hysteresis loops of the microspheres obtained from powder and fluid phase, respectively. The saturation magnetization (M_s) value of the microspheres gradually increased with increasing R, which should be mainly attributed to the increase of γ-Fe_2O_3 NPs fraction in each microsphere. Magnetization curves with no

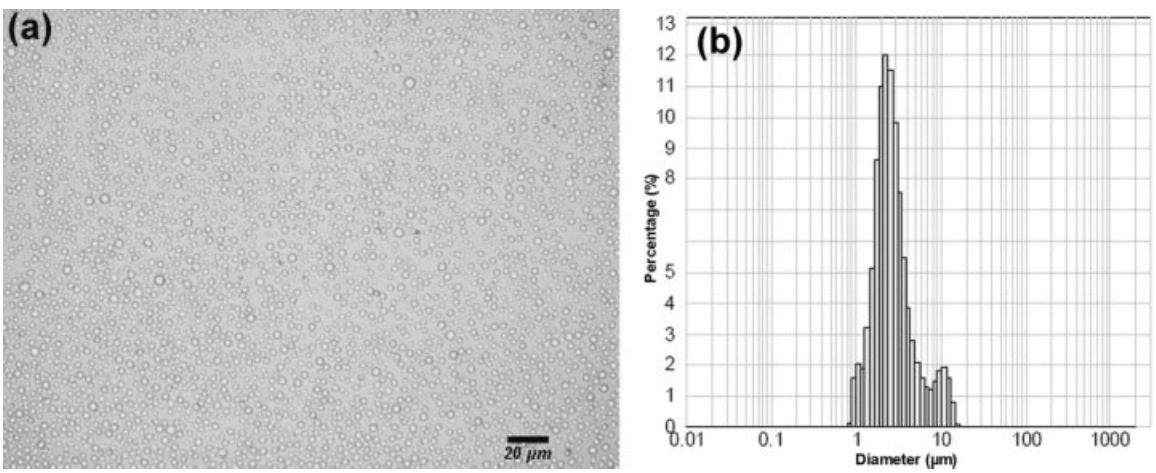

Figure 6 Optical microscopy image of the composite alginate microspheres and the corresponding diameter distribution. The synthetic parameters were as follows: R (0.2), HLB value (5), stirring speed (600 rpm), and $CaCl_2$ dripping rate (60 mL· h^{-1}).

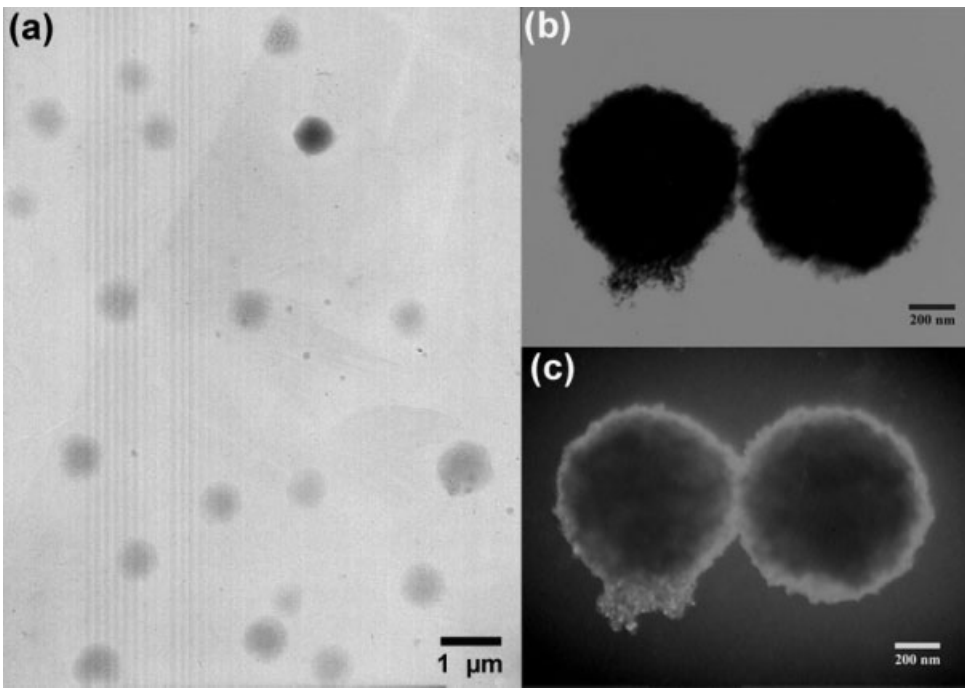

Figure 7 Typical TEM bright-field (a and b) and dark-field (c) images of the composite microspheres.

remanence or coercivity at room temperature indicate a superparamagnetic behavior. A typical M_s of the microspheres (15.9 emu/g), is much less than that of γ-Fe_2O_3 (50.9 emu/g) and γ-Fe_2O_3@DMSA NPs (47.7 emu/g), which could be explained by the diamagnetic contribution of the alginate matrix surrounding the magnetic cores. This result implies at least 32 wt % of γ-Fe_2O_3 NPs in the microspheres, which is much higher than that of magnetic alginate composites reported previously.[25,39] Moreover, the magnetic separability of the microspheres was tested by placing an external magnetic field near the glass bottle. The microspheres were attracted toward the magnet within 20 s [see inset in Fig. 8(b)], demonstrating that they have strong magnetic responses to an external magnetic field. And this presents an easy and an efficient way to separate the microspheres from a suspension system under an external magnetic field.

Figure 9 shows the typical fluorescence spectrum of the composite microspheres, which is similar to the spectrum of free FITC molecules but with a

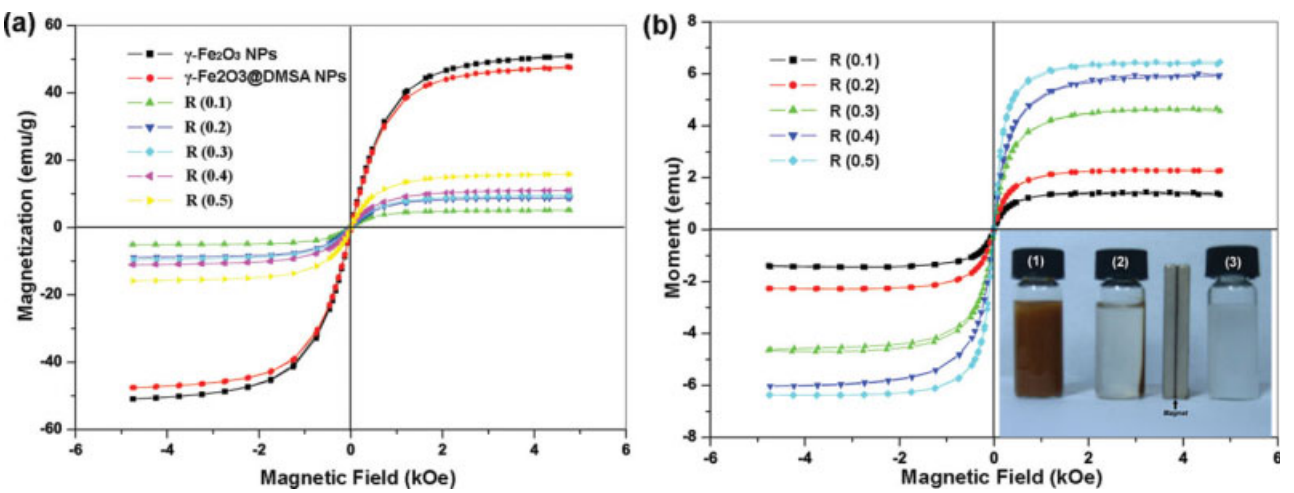

Figure 8 Room temperature hysteresis loops of the samples obtained from powder (a) and fluid (b) form. The measured samples in fluid form were all dispersed into water with the same alginate concentrations of 12.5 mg/mL and 75-μL aliquot of each sample was determined using VSM. The inset in (b) shows photographic image of the composite alginate microspheres in the absence (1) and presence (2) of an external magnet and pure alginate microspheres (3) in the presence of the magnet. [Color figure can be viewed in the online issue, which is available at www.interscience.wiley.com.]

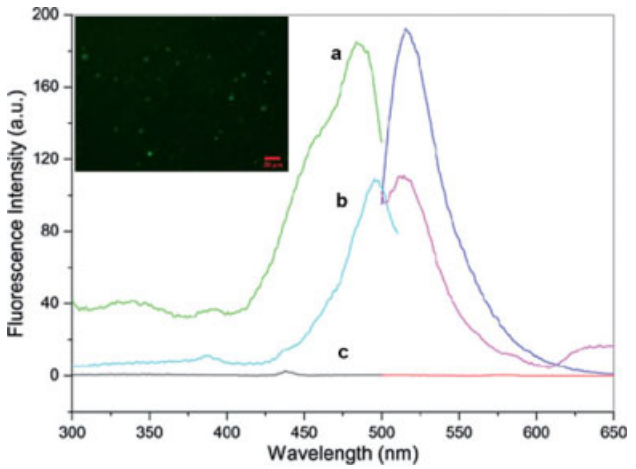

Figure 9 Excitation and emission spectra of free FITC (a), composite microspheres (b), and water (c). The inset shows a typical fluorescence image of composite alginate microspheres spread on a glass surface. [Color figure can be viewed in the online issue, which is available at www.interscience.wiley.com.]

small blue shift of fluorescence emission peak. The small blue shift resulted from the interaction between the isothiocyanate groups of FITC and the amino groups of alginate-amine derivative. The quantum yield value of the composite microspheres was approximately 0.16, much less than that of pure FITC (~0.95) and alginate-FTIC derivative (~0.89). This profound fluorescence quenching effect may be due to the nonradiative energy transfer between the FITC and the magnetic NPs.[40] However, there is sufficient fluorescence intensity for tracing of the microspheres by fluorescence microscopy (Fig. 9). And this will provide a visual detection method for cell labeling.

Fluorescent and MRI detection of cells labeled with composite alginate microspheres

To evaluate the fluorescent and MRI detection of the labeled cells, RAW264.7 cells were labeled with various concentrations of composite alginate microspheres. In control experiments, medium having no particles was used. Using a clinical 1.5 T imager, T_2* -weighted MR images of samples in Eppendorf tubes were obtained. As shown in Figure 10, cells incubated with the composite alginate microspheres exhibit significant negative contrast enhancement with increasing concentration when compared with control of water and unlabeled cells. It has been reported that micrometer-sized polymer microspheres containing iron oxide core are highly effective T_2* contrast agents for detection of single cells.[41,42] The utilization of larger particles containing higher quantities of Fe_3O_4 or γ-Fe_2O_3 may provide higher iron uptake and sensitivity even if cellular

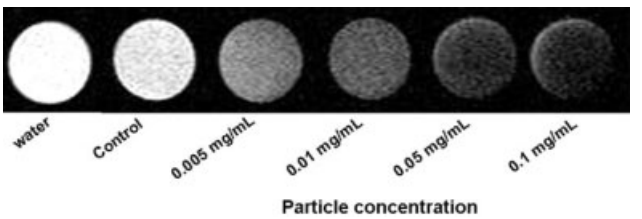

Figure 10 T_2*-weighted spin-echo MR images of cells when labeled with composite alginate amicrospheres with various concentrations *in vitro*.

incorporation of particles is numerically lower.[43] The microspheres described here potentially can serve as an efficient MR contrast agent for detection of cells. Moreover, fluorescence microscopic studies indicated the FITC fluorescence is clearly visible in the fluorescent image of cells incubated with 0.05 mg/mL composite alginate microspheres for 2 h but completely absent in the fluorescent image of cells alone (Fig. 11). Hence, FITC molecules coupled onto the microspheres enabled their direct imaging by fluorescence microscopy.

To evaluate the biocompatibility of the composite alginate microspheres as imaging probes, we

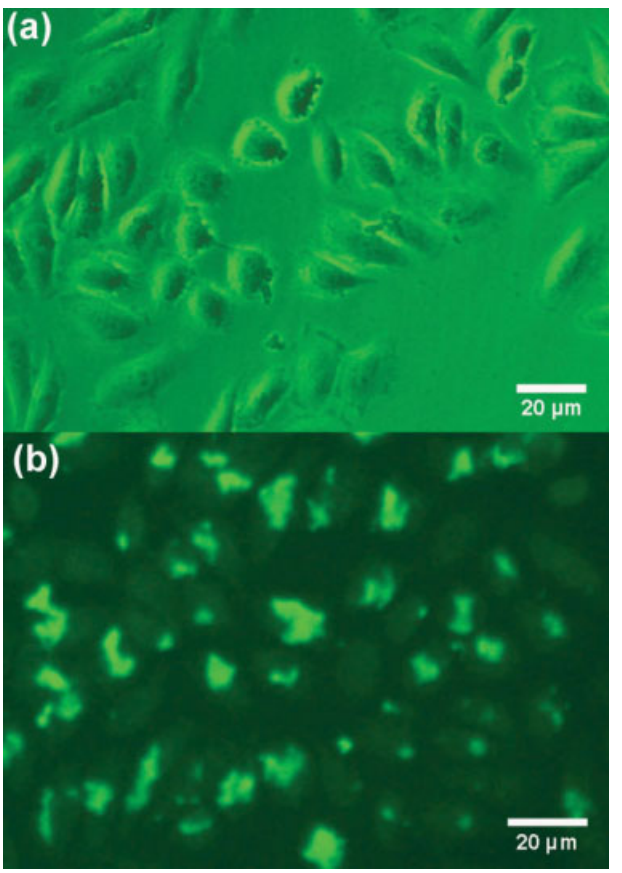

Figure 11 Fluorescent image of control (a) and cells incubated with 0.05 mg/mL composite alginate microspheres for 2 h (b). [Color figure can be viewed in the online issue, which is available at www.interscience.wiley.com.]

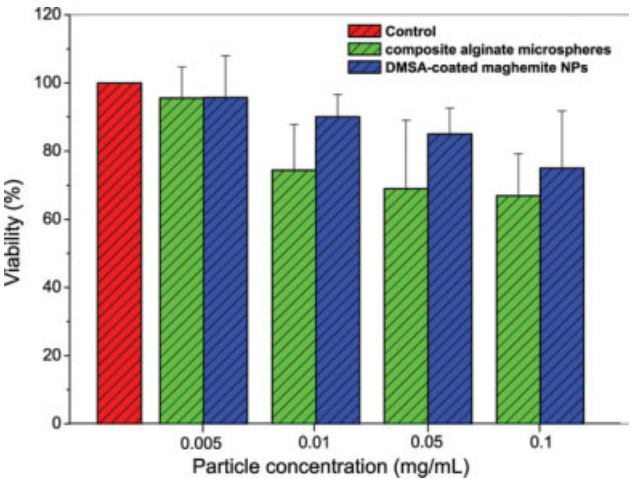

Figure 12 Viability of the cells when incubated with γ-Fe_2O_3@DMSA NPs and composite alginate microspheres as determined by MTT assay. [Color figure can be viewed in the online issue, which is available at www.interscience.wiley.com.]

investigated the cytotoxicity of the microspheres using MTT assay. It was previously reported that iron oxide NPs have no significant cytotoxicity up to 0.1 mg/mL.[44] Figure 12 shows that there is no significant difference in cell viability of the microspheres treated cells as compared to the cells treated with γ-Fe_2O_3@DMSA NPs, when tested at the lowest concentration (0.005 mg/mL). And even when tested at higher concentration (0.1 mg/mL), the microspheres caused a reduction (70% of control) in cell viability. It seemed that the composite alginate microspheres are biocompatible and safe for biomedical purposes.

CONCLUSIONS

Composite alginate microspheres with magnetic and fluorescent functionalities have been successfully synthesized via an emulsification technique. The results show the synthetic parameters including the weight ratio of DMSA-coated maghemite NPs to alginate, HLB value, stirring speed, and $CaCl_2$ dripping rate play important roles in the synthesis of microspheres. Moreover, the microspheres described here can serve both as magnetic resonance contrast agents for MRI and optical probes for fluorescence microscopy, which will have great potential in a variety of biological and biomedical applications.

References

1. Smith, J. E.; Medley, C. D.; Tan, W. H. Anal Chem 2007, 79, 3075.
2. Berry, C. C.; Wells, S.; Charles, S. Biomaterials 2003, 24, 4551.
3. Kim, D. K.; Muhammed, M. J Magn Magn Mater 2001, 225, 256.
4. Lee, H.; Lee, E.; Jon, S. J Am Chem Soc 2006, 128, 7383.
5. Neuberge, T.; Hofmann, M. J Magn Magn Mater 2005, 293, 483.
6. Jordan, A.; Felix, R. J Magn Magn Mater 1999, 194, 185.
7. Kim, D. K.; Mikhaylova, M.; Zhang, Y. Chem Mater 2003, 15, 1617.
8. Zaitsev, V. S.; Filimonov, D. S.; Chu, B. J Colloid Interf Sci 1999, 212, 49.
9. Fauconnier, N.; Bee, A.; Roger, J.; Pons, J. N. J Mol Liq 1999, 83, 233.
10. Wang, Y.; Teng, X. W.; Wang, J. S.; Yang, H. Nano Lett 2003, 3, 789.
11. Chatterjee, J.; Haik, Y.; Chen, C. J. J Magn Magn Mater 2002, 246, 382.
12. Xu, H.; Cui, L. L.; Tong, N. H.; Gu, H. C. J Am Chem Soc 2006, 128, 15582.
13. Peniche, H.; Osorio, A.; Acosta, N.; Peniche, C. J Appl Polym Sci 2005, 98, 651.
14. An, X. N.; Su, Z. X.; Zeng, H. M. J Chem Technol Biotechnol 2003, 78, 596.
15. Chatterjee, J.; Haik, Y.; Chen, C. J. Colloid Polym Sci 2001, 279, 1073.
16. Gombotz, W. R.; Wee, S. F. Adv Drug Deliv Rev 1998, 31, 267.
17. Lee, K. Y.; Mooney, D. J. Chem Rev 2001, 101, 1869.
18. Kuo, C. K.; Ma, P. X. Biomaterials 2001, 22, 511.
19. Muraoka, M.; Hu, Z. P.; Takada, K. J Control Release 1998, 52, 119.
20. George, M.; Abraham, T. E. J Control Release 2006, 114, 1.
21. Rowley, J. A.; Madlambayan, G.; Mooney, D. J. Biomaterials 1999, 20, 45.
22. Kroll, E.; Winnik, F. M. Chem Mater 1996, 8, 1594.
23. Llanes, F.; Ryan, D. H.; Marchessault, R. H. Int J Biol Macromol 2000, 27, 35.
24. Finotelli, P. V.; Morales, M. A.; Rossi, A. M. Mat Sci Eng C Bio Sci 2004, 24, 625.
25. Morales, M. A.; Finotelli, P. V.; Rossi, A. M. Mat Sci Eng C Bio Sci 2008, 28, 253.
26. Safarikova, M.; Safarik, I. J Biotechnol 2003, 105, 255.
27. Teotia, S.; Gupta, M. N. Mol Biotechnol 2002, 20, 231.
28. Shen, F.; Somers, S.; Chang, P. L. Biotechnol Bioeng 2003, 83, 282.
29. Rocher, V.; Siauque, J. M.; Bee, A. Water Res 2008, 42, 1290.
30. Salgueirino-Maceira, V.; Farle, M. Adv Funct Mater 2006, 16, 509.
31. Deng, Y. H.; Yang, W. L.; Fu, S. K. Adv Mater 2003, 15, 1729.
32. Sun, Y. K.; Zhang, Y.; Gu, N. Colloid Surf A 2004, 245, 15.
33. Zhang, S.; Gu, N.; Zhang, J. N. Colloid Surf B 2007, 55, 143.
34. Zhu, H. G.; Mcshane, M. J. Bioconjugate Chem 2005, 16, 1451.
35. Zhu, H. G.; Srivastava, R.; Mcshane, M. J. Biomacromolecules 2005, 6, 2221.
36. Srivastava, R.; Brown, J. Q.; Mcshane, M. J. Biotechnol Bioeng 2005, 91, 124.
37. Srivastava, R.; Brown, J. Q.; Mcshane, M. J. Macromol Biosci 2005, 5, 717.
38. Cumberland, S. L.; Hanif, K. M.; Yun, C. S. Chem Mater 2002, 14, 1576.
39. Boissiere, M.; Allouche, J.; Coradin, T. Int J Pharm 2007, 344, 128.
40. Josephson, L.; Kircher, M. F.; Weissleder, R. Bioconjugate Chem 2002, 13, 554.
41. Hinds, K. A.; Hill, J. M.; Dunbar, C. E. Blood 2003, 102, 867.
42. Wu, Y. L.; Ye, Q.; Williams, J. B.; Ho, C. PNAS 2006, 103, 1852.
43. Williams, J. B.; Ye, Q.; Ho, C. J Magn Reson Imaging 2007, 25, 1210.
44. Sonvico, F.; Mornet, S.; Couvreur, P. Bioconjugate Chem 2005, 16, 1181.